

A new method for faster and more accurate inference of species associations from novel community data

Maximilian Pichler^{1,*}, Florian Hartig¹

¹ Theoretical Ecology, University of Regensburg, Universitätsstraße 31, 93053 Regensburg, Germany

*corresponding author, maximilian.pichler@biologie.uni-regensburg.de

Keywords:

machine learning, regularization, metacommunity, co-occurrence, deep learning, big data

Abstract

Joint Species Distribution models (jSDMs) explain spatial variation in community composition by contributions of the environment, biotic interactions, and possibly spatially structured residual variance. They show great promise as a general analysis method for community ecology and macroecology, but current jSDMs scale poorly on large datasets, limiting their usefulness for novel community data, such as datasets generated using metabarcoding and metagenomics. Here, we present sjSDM, a novel method for estimating jSDMs that is based on Monte-Carlo integration of the joint likelihood. We show that our method, which can be calculated on CPUs and GPUs, is orders of magnitude faster than existing jSDM algorithms and can be scaled to very large datasets. Despite the dramatically improved speed, sjSDM produces the same predictive error and more accurate estimates of species association structures than alternative jSDM implementations. We provide our method in an R package to facilitate its applicability for practical data analysis.

Introduction

Understanding the spatial structure and assembly of ecological communities is a central concern for ecology, biogeography and macroecology. The question is tightly connected to many important research programmes of the field, including coexistence theory (e.g. Levine *et al.* 2017) or understanding ecosystem responses to global change (Urban *et al.* 2016).

Spatial community data is currently analyzed in two major theoretical frameworks: metacommunity theory (see Leibold *et al.* 2004) and species distribution models (SDMs, Elith & Leathwick 2009). Metacommunity theory formed in the last two decades as the study of the spatial processes that give rise to regional community assembly (e.g. Leibold *et al.* 2004; Leibold & Chase 2017). The current analytical framework of metacommunity ecology is based on statistical variation partitioning, which disentangles abiotic and spatial contributions to community assembly (see Cottenie 2005; Leibold & Chase 2017). SDMs are statistical models that link abiotic covariates to species occurrences. They are widely used in spatial ecology, for example to study invading species (Gallien *et al.* 2012; Mainali *et al.* 2015) or species responses to climate change (Thuiller *et al.* 2006).

A key limitation of both variation partitioning and SDMs, noted in countless studies, is that they do not account for species interactions. Both approaches essentially assume species that depend only on space and the environment (Cottenie 2005; Peres-Neto & Legendre 2010; Dormann *et al.* 2012; Wisz *et al.* 2013), whereas in reality we know that species also influence each other through competition, predation, facilitation and other processes (Gilbert & Bennett 2010; Van der Putten *et al.* 2010; see Mittelbach & Schemske 2015; see Leibold & Chase 2017).

Joint Species Distribution Models (jSDM) recently emerged as a novel analytical framework that could integrate species interactions into metacommunity and macroecology. jSDM are

similar to SDMs in that they describe species occurrence as a function of the environment, but they also consider the influence of species-species associations (see, e.g., Pollock *et al.* 2014, Dormann *et al.* 2018). Whether those association originate from “true” biotic interactions (e.g. competition, predation, parasitism, mutualism) or other reasons needs to be carefully considered (see Dormann *et al.* 2018), but when appropriately interpreted, jSDMs combine the essential processes believed to be responsible for the assembly of ecological communities: environment, space, and biotic interactions, and they could be adjusted to work for large-scale as well as for metacommunity analyses (e.g. Gilbert & Bennett 2010; Mittelbach & Schemske 2015; Leibold & Chase 2017)

Interest in jSDMs is further fueled by the emergence of high-throughput technologies that are currently revolutionizing our capacities for observing community data (e.g. Pimm *et al.* 2015). We can now detect hundreds or even thousands of species from environmental DNA (eDNA) or bulk-sampled DNA (Cristescu 2014; Deiner *et al.* 2017; see also Bálint *et al.* 2018; Humphreys *et al.* 2019; Tikhonov *et al.* 2019a) in a given sample, and next generation sequencing (NGS) has become cheap enough that this process could be replicated at scale. Moreover, there are also other emerging technologies that could produce large amounts of community data in the future, for example automatic species recognition (Guirado *et al.* 2018; e.g. Tabak *et al.* 2019) from acoustic recordings; for example of fish (see Desjonquères *et al.* 2019.; e.g. Picciulin *et al.* 2019), forest wildlife (e.g. see Wrege *et al.* 2017), bird communities (Fritzler *et al.* 2017; Lasseck 2018; Wood *et al.* 2019) or bats (e.g. Mac Aodha *et al.* 2018). Jointly, these developments mean that large spatial community datasets will become available in the near future, and ecologists have to consider how to best analyze them.

Joint species distribution models would seem the natural analytical approach for these emerging new data, given their ability to separate the processes essential for spatial community assembly. Current jSDM software, however, have severe limitations for processing such large datasets. Most existing jSDMs are based on the multivariate probit model (MVP,

Chib & Greenberg 1998), which describes species-species associations via a covariance matrix (e.g. Ovaskainen *et al.* 2010; Clark *et al.* 2014; Pollock *et al.* 2014; Golding *et al.* 2015; Hui 2016). The limitation of the MVP approach is that it scales poorly for species-rich data, as the number of parameters in the species-species covariance matrix increases quadratically with the number of species (see Warton *et al.* 2015). The current solution to this problem are latent-variable model (LVM), which replace the covariance matrix with a small number of latent variables (see Warton *et al.* 2015).

The LVM approach is computationally more efficient than the full MVP, while still allowing to model abiotic preferences and biotic species-species associations (see Warton *et al.* 2015; Ovaskainen *et al.* 2017; Tikhonov *et al.* 2017; Niku *et al.* 2019; Norberg *et al.* 2019; Tikhonov *et al.* 2019a). That, however, does not mean that these models are fast. Integrating out the latent variables requires MCMC sampling or numerical approximations (e.g. Laplace, variational inference, see Niku *et al.* 2019), which is computationally costly and can fail to converge. For communities with hundreds of species, computational runtimes of current LVMs can still exceed hours or days (e.g. Tikhonov *et al.* 2019a; Wilkinson *et al.* 2019). This poses severe limitations for analyzing eDNA data, which can include thousands of species or OTUs (e.g. Frøslev *et al.* 2019). Moreover, LVMs also scale disadvantageously with the number of sites, because each site introduces a weight in the latent variables (Skrondal & Rabe-Hesketh 2004; Bartholomew *et al.* 2011). With increasing numbers of sites (on the order of thousands), the advantage of the LVM over the MVP is reduced. An important challenge for the field is therefore to make jSDMs fast enough for big datasets (Krapu & Borsuk 2020).

A second question for jSDM development is the accuracy of inferred species associations. Surprisingly little is known about this question. Most existing jSDM assessments (e.g. Norberg *et al.* 2019; e.g. Tobler *et al.* 2019; Wilkinson *et al.* 2019) concentrate on runtime, predictive performance, or on aggregated measures of accuracy that do not necessarily capture the error

of the estimated species-association structure. From a statistical perspective, it is clear that estimating a large species covariance matrix with a limited data must have considerable error.

The LVM approach reduces the degrees of freedom in the covariance (even with hundreds of species, the number of latent variables is not raised higher than 32, see Tikhonov *et al.* 2019a). As for all regularization approaches, this should reduce the statistical error on the covariance estimates, but possibly at the cost of creating some bias. Moreover, the structure induced by the LVM will likely not favor sparse covariance matrices. This is of particular concern for high-throughput technologies, because those detect species already at very low densities, leading to large species list. It is ecologically unlikely that all those species have associations, and in particular rare and common species might have different interaction structures (Calatayud *et al.* 2019). Whether the LVM approach is beneficial for making species association estimates with low error in this setting, especially in comparison to other options, has not yet been investigated.

Here, we propose a new jSDM algorithm that addresses many of the above-mentioned problems. Our method is based on the standard multivariate probit model, without latent variables. To solve the problem of computational speed, we use a Monte-Carlo approach (originally proposed by Chen *et al.* 2018) that can be outsourced to graphical processing units (GPUs), which makes model fitting extremely fast. To address the issue of variance in the estimates and overfitting, we introduce a new regularization approach, which directly targets the covariance matrix of the MVP model.

In the remainder of this paper, we introduce the approach in detail, and assess: (i) the computational runtime on GPUs and CPUs (ii) the inferential performance for the species-species covariance matrix and the environmental species responses and (iii) the predictive performance of our model. For comparison with existing solutions, we use the state-of-the-art jSDM software packages Hmsc, glvm, and BayesComm, as well as results from a recent

jSDM model comparison (Wilkinson *et al.* 2019). Finally, to illustrate the applicability of our approach to large eDNA community data, we additionally applied our model to a community dataset containing 5,564 species.

Methods

The structure of the jSDM problem

Before discussing individual jSDM implementations, it is useful to give a precise description of the jSDM problem. Our goal is to simultaneously estimate how the environment (i.e species' niches) and species-species associations affect local community composition.

Species-environment associations are classically addressed by species distribution models (SDM), which estimate the probability of abundance or presence of a species as a function of some the environmental predictors. The functional form of the niche can be expressed by GLMs, or by more flexible approaches such as generalized additive models, boosted regression trees or Random Forest (see Elith & Leathwick 2009).

A jSDM generalizes this approach by including the possibility of species-species associations. By an association, we mean that two species tend to appear together more or less often than expected from their environmental responses alone. The most common structure that has emerged to fit species associations is the multivariate probit model, which describes the site by species matrix y_{ij} as a function of the environment, plus a multivariate normal distribution that describes the species-species associations:

$$probit(y_{ij}) = \beta_{0j} + X_{in} * \beta_{nj} + MVN(0, \Sigma_{jj}) \quad (1)$$

After the model is fit, the fitted species-species covariance matrix σ is normally transformed into a correlation matrix for further interpretation.

Current approaches to fit the jSDM model structure

The model structure described in eq. 2 can be fit directly, using logit (Ovaskainen *et al.* 2010) or probit links, and the first jSDM studies used this approach (Chib & Greenberg 1998; Pollock *et al.* 2014; see Wilkinson *et al.* 2019). Fitting the MVP model directly, however, has two drawbacks: first, calculating likelihoods for large covariance matrices is computationally costly. Second, the number of parameters in the covariance matrix for j species increases quadratically as $(j*(j-1)/2)$, i.e. for 50 species there are 2250 parameters to fit.

Because of these problems, a series of papers (Warton *et al.* 2015; Ovaskainen *et al.* 2016) introduced the latent-variable model (see Skrondal & Rabe-Hesketh 2004) to the jSDM problem. The idea of latent-variable jSDMs is to replace the covariance matrix by some latent variables, on which the species depend additionally to the real predictors (these latent dependencies are often called factor loadings). Species that react (via their factor loadings) similarly or differently to the latent variables thus show positive or negative associations, respectively (see Warton *et al.* 2015; see Ovaskainen *et al.* 2017; see Wilkinson *et al.* 2019 for details). The factor loadings can be translated into a species-species covariance matrix: $\Sigma_{j,j} = \lambda_{jl} * \lambda_{jl}^T$ (λ = factor loadings), allowing the model to effectively fit species associations. The latent variables are sometimes interpreted as unobserved environmental predictors, but in general, they are probably better viewed as a purely technical construct that amounts to a regularized reparameterization of the covariance matrix. The complexity of association structure can be set via the number of latent variables (usually to a low number, see Warton *et al.* 2015)

An alternative approach to fit the jSDM structure

Because the latent-variable models still have computational limitations, and also because of the need for flexible regularization discussed in the introduction, we propose a different approach to fit the model structure in eq. 1. The main computational issue of the multivariate probit models is that the cumulative multivariate normal distribution has no closed analytical expression, which makes the evaluation of the likelihood costly. Chen *et al.* 2018 proposed a solution to this issue by parallel sampling under the assumption that the residuals are normally distributed. In their study, Chen *et al.* 2018 used this idea to approximate the multivariate joint likelihood using a deep neural network (see LeCun *et al.* 2015).

Here, we use the same idea, but apply it to the standard generalized linear multivariate probit model, which means that we conform to the model structure typically used in this field and can profit from all benefits associated with parametric models. We implemented the method in an R package (see section Data Accessibility), using PyTorch (Paszke *et al.* 2017) and reticulate (Ushey *et al.* 2019), which allows calculations to be performed on a computer's GPU.

Outsourcing the Monte-Carlo approach to a GPUs solves the issue of computational speed (as we show below), but it does not yet solve the problem that the covariance matrix has a very large number of parameters, which raises the problem of overfitting when the method is used on small datasets. To address this, we penalized the actual covariances in the species-species covariance matrix with a combination of ridge and lasso penalty (elastic net, see Zou & Hastie 2005, more details below).

Benchmarking our method against state-of-the-art jSDM implementation

To benchmark our approach, we used six datasets from Wilkinson *et al.* 2019, a recent jSDM benchmark study (Table 1). Covariates were centered and standardized. Using this data has the advantage that we can also compare our results to Wilkinson *et al.* 2019.

Additionally, we simulated new data from a multivariate probit model (eq 2), varying the number of sites from 50 to 500 (50, 70, 100, 140, 180, 260, 320, 400, 500) and the number of species as a percentage (10%, 30% and 50%) of the sites (e.g. the scenario with 100 sites and 10% results in 10 species). In all simulations, the species' environmental preference was described for five environmental covariates (beta), which was randomly selected. For each scenario, we simulated 10 communities. Here, all species had species-species associations, i.e. the species-species covariance matrices were not sparse (for details, see Supporting Information S1).

Table 1: Compiled datasets that were taken from Wilkinson *et al.* 2019

| Dataset | Original paper | Species | Sites | Covariates |
|-------------|-------------------------------|---------|-------|------------|
| Birds | Harris 2015 | 370 | 2,752 | 8 |
| Butterflies | Ovaskainen <i>et al.</i> 2016 | 55 | 2,609 | 4 |
| Eucalypts | Pollock <i>et al.</i> 2014 | 12 | 458 | 7 |
| Frogs | Pollock <i>et al.</i> 2014 | 9 | 104 | 3 |
| Fungi | Ovaskainen <i>et al.</i> 2010 | 11 | 800 | 15 |
| Mosquitos | (Golding 2015) | 16 | 167 | 13 |

To compare our model to existing jSDM software packages, we selected BayesComm (version 0.1-2, Golding & Harris 2015), the fastest non-latent multivariate probit model according to Wilkinson *et al.* (2019), and two state-of-the-art latent-variable jSDM implementations: Hmsc (version 3.0-4, Tikhonov *et al.* 2019b), which uses MCMC sampling, and gllvm (version 1.2.1, Niku *et al.* 2020), which uses variational Bayes and Laplace approximation to fit the model. Parameter settings for all three methods were in line with other recent jSDM benchmarks (details see Supporting Information S1).

To assess the predictive performance of the models, we calculated the average area under the curve (AUC) over all species and 10 independent replicates for each scenario. To calculate the accuracy of the estimated species associations and environmental coefficients, we used root mean squared error and the accuracy of the coefficients' signs, again averaged over all species and replicates.

Regularization to infer sparse species-species associations

For the previous benchmark, we simulated data under the assumption that all species interact. While this assumption may or may not be realistic, it is generally desirable for a method to work well also when there is only a small number of associations, i.e. when the species-species covariance matrix is sparse. We were particularly interested in this question because we conjectured that the LVM approach imposes correlations on the species-species associations that makes it difficult for LVM models to fit arbitrarily sparse covariance structures.

We therefore simulated the same scenarios, but with 50% sparsity in the species-species covariance matrices. To adjust our model to such a sparse structure, we applied an elastic net shrinkage (Zou & Hastie 2005) with $\alpha = 0.5$ on all off-diagonals of the covariance matrix.

Following common practice, the penalty term was tuned for each scenario from 18 different lambdas. For BayesComm, glvm, and Hmsc, we used the default settings (see details and additional comments in Supporting Information S1).

To measure the accuracy of inferred species-species associations for this benchmark, we normalized the covariance matrices to correlation matrices and calculated AUCs for the three different classes (zero – non-zero(positive/negative), positive – non-positive (zero/negative), negative – non-negative (zero/positive)), which we weighted after the overall class distributions (for 50% sparsity, we get 50% zeros, 25% positive and 25% negative values), and summed the weighted AUCs to get the average AUC.

Case study – Inference of species-species associations from eDNA

To demonstrate the practicability of our approach, we fit our model to an eDNA community dataset from a published study that sampled 130 sites across Denmark (for details on the study design see Brunbjerg *et al.* 2017; for data and bioinformatics see Frøslev *et al.* 2019). On each site, eight environmental variables were recorded: precipitation, soil pH, soil organic matter, soil carbon content, soil phosphorous content, and mean Ellenberg values (light condition, nutrient status, and soil moisture) based on the plant community. Frøslev *et al.* 2019 identified by eDNA sequencing (81 samples per site) 10,490 species. We followed Frøslev *et al.* 2019 and removed five sites with the most redundant species. We used only species occurring at least two times over the remaining 125 sites, which reduced the overall number of species from 10,490 to 5,564 species. All eight environmental variables were used in our analysis. The final dataset consisted of 5,564 species co-occurrences over 125 sites with 8 environmental variables.

We used again elastic net with $\alpha = 0.5$ for the regularization of the z-transformed environmental predictors and the covariances of the species-species associations. We varied the regularization strength from $3.8\text{e-}6$ to 0.5 in 30 steps. In each step, we fit a G-sjSDM model in 50 epochs, 5564×2782 weights for the covariance matrix, with batch size of 8 and learning rate of 0.001. The sampling iteration parameter was set to 100.

Results

Method validation and benchmark against state-of-the-art

jSDMs

Computational speed

On a GPU, our approach (G-sjSDM) required under 3 seconds runtime for any of our simulations. When run on CPUs only (C-sjSDM), runtimes increased to a maximum of around 2 minutes (Fig. 1a, Fig. S1). Hmsc had a runtime of around 7 minutes for our smallest scenario and increase in runtime exponentially when the number of species exceeded 40 (Fig. 1a). BayesComm was slightly faster than Hmsc for small problems but had the worst scaling for larger data. glvm achieved fast runtimes, on par and sometimes better than our method for less than 50 species, but beyond that runtime started to increase exponentially as well, leading to runtimes >10 min for our larger test cases (Fig. 1a).

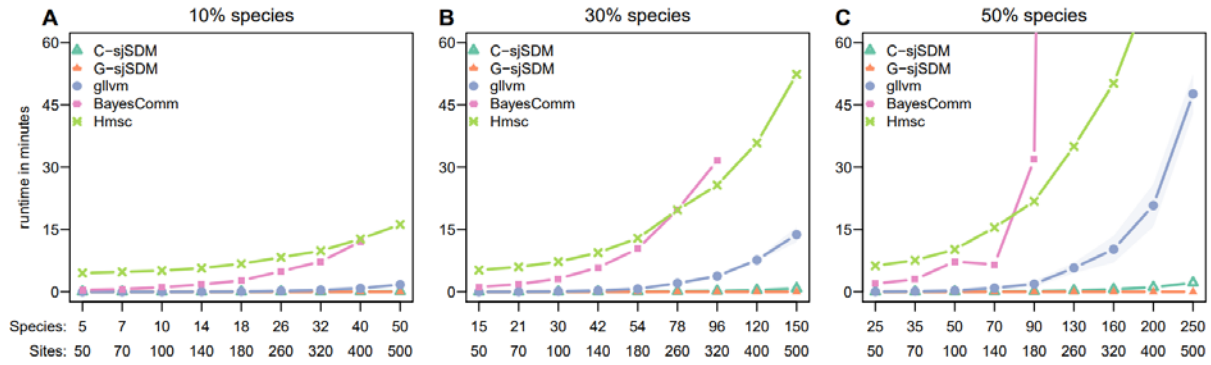


Figure 1: Results for runtime benchmarks of G-sjSDM, C-sjSDM, gllvm, BayesComm, and Hmsc. Models were fit to different simulated scenarios: 50 to 500 sites with 10% (a), 30% (b) and 50% (c) number of species (e.g. for 100 sites and 10% we get 10 species). For each scenario, ten datasets were simulated and analyzed, and results were averaged. BayesComm was aborted for some scenarios due to too long runtimes.

Because of the runtime limitations of the other approaches, we calculated large-scale scenarios only for G-sjSDM. Going from 5,000 to 32,000 sites increased runtimes from 7-15 seconds to 60-80 seconds (Fig. 2). G-sjSDM showed greater (but sub-exponential) runtime increases when increasing numbers of sites, while the numbers of species had only small effects on runtimes (Fig. 2).

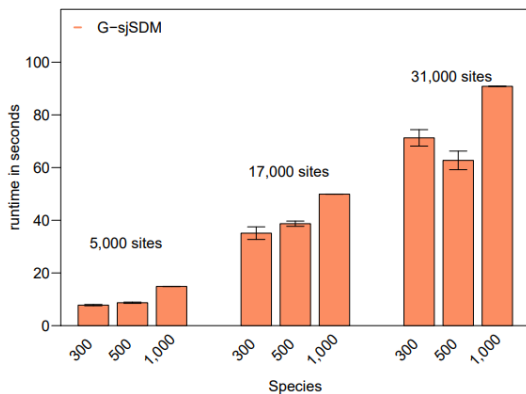


Figure 2: Benchmark results for sjSDM on big community data. We simulated communities with 5,000 – 31,000 sites and for each 300, 500, and 1,000 species.

For the datasets from Wilkinson *et al.* (2019), the CPU based C-sjSDM model achieved a 4.75 times lower runtime for the bird dataset and 230 times lower runtime for the butterfly dataset than MLP (which corresponds to BayesComm), the fastest jSDM in Wilkinson *et al.* 2019. The G-sjSDM run on the GPU achieved a 3800 times lower runtime for the bird dataset and a 230 times lower runtime for the butterfly dataset than did MLP, the previously fastest model (Table 2).

Table 2: Model runtimes in hours. Results for MPR, MLR, HPR, LPR, DPR, HLR-S, HLR-NS taken from (Wilkinson *et al.* 2019).

| Dataset | Wilkinson et al. 2019 | | | | | | | Our framework | |
|-------------|-----------------------|-------|------|-------|------|-------|--------|------------------|------------------|
| | MPR | MLR | HPR | LPR | DPR | HLR-S | HLR-NS | C-sjSDM | G-sjSDM |
| Birds | 3.8 | >168 | NA | 120.4 | 27.3 | >168 | 15.2 | 0.8 | <0.001 |
| Butterflies | 0.23 | >168 | >168 | 13.9 | 6.5 | >168 | 2.1 | <0.001 | <0.001 |
| Eucalpyts | <0.02 | 142.1 | 7.6 | 0.33 | 0.25 | 50.0 | 0.21 | <0.001 | <0.001 |
| Frogs | <0.02 | 14.1 | 0.94 | 0.04 | 0.06 | 1.4 | 0.13 | <0.001 | <0.001 |
| Fungi | <0.02 | >168 | 15.8 | 0.62 | 0.67 | NA | 0.26 | <0.001 | <0.001 |
| Mosquitos | <0.02 | >168 | 6.4 | 0.14 | 0.73 | 2.0 | 0.2 | <0.001 | <0.001 |

Accuracy of the inference about species-environment and species-species associations

For scenarios with dense association structures, BayesComm and sjSDM consistently achieved higher accuracy in the inferred species-species associations than the LVM models Hmsc and gllvm (Fig. 3 a). The performance of all methods dropped with an increasing proportion of species, to around 70% for the non-latent and 60% for the LVM models (Fig. 3 a). The LVM models gllvm and Hmsc also showed lower inferential performance for environmental preferences (measured by RMSE) when the number of sites was low (Fig. S2b), while all models performed approximately equal for a high number of sites (Fig. S2b).

For sparse species-species covariance matrices, sjSDM achieved the highest AUC (between 0.7 to 0.85 AUC, see Fig. 3b). gllvm and HSMC achieved on average 0.1 AUC less, with a stronger decrease in performance as the number of species increased (Fig. 3b). BayesComm,

which worked well for dense species-species associations, performed poorly in this benchmark, with an AUC of approximately 0.5 in all sparse scenarios (Fig. 3b). The inferential performance regarding the environmental predictors showed the same pattern as for dense species-species associations, except for gllvm. All models improved their environmental accuracy (Fig. S2c) and reduced RMSE as the number of sites increased (Fig. S2d). Only gllvm performed significantly worse, with an accuracy of 0.5 – 0.55 and on average four times higher RMSE error than for the other models (Fig. S2d).

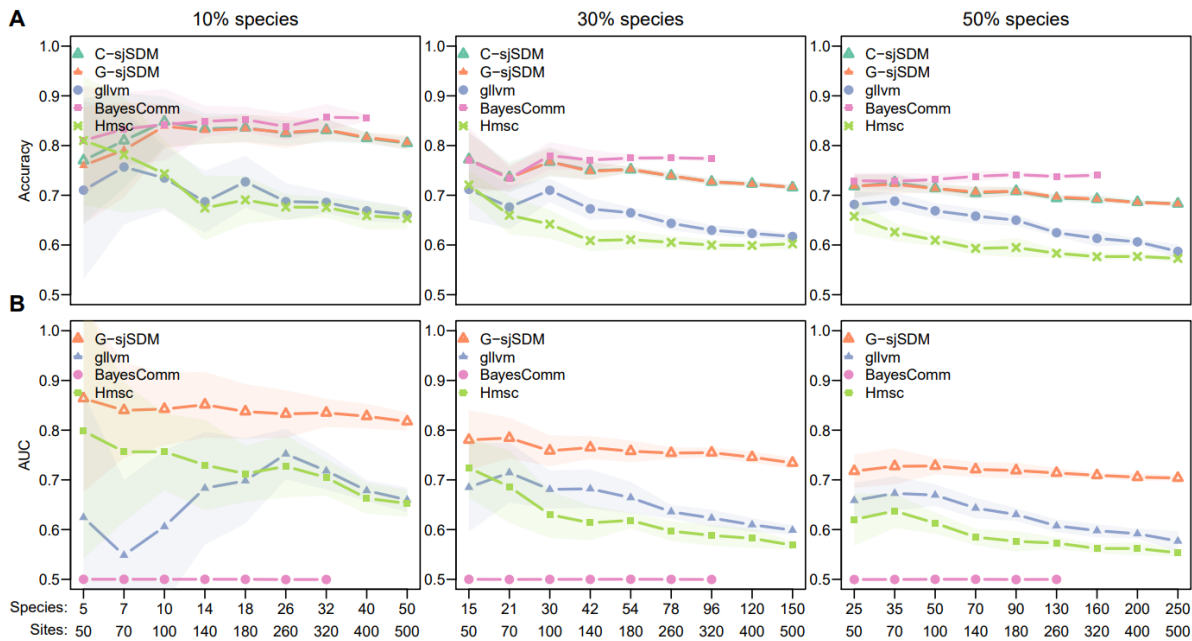


Figure 3: Accuracy of the inferred environmental responses and species-species associations. Models were fit to simulated data with 50 to 500 sites and the number of species set to 0.1, 0.3 and 0.5 times the number of sites. All values are averages from 10 simulated datasets. Due to high runtimes, runs for BayesComm were aborted at specific points. The upper row shows the accuracies of matching signs (positive or negative covariance) for the estimated and true species-species association matrix. The lower row shows the accuracy of inferred species associations for sparse association matrices (50% sparsity), measured by weighted AUCs for the multi-label classification problem: zero, positive, and negative.

Predicting species occurrences

Predictions of all models performed similarly in the simulation scenarios with around 0.75 AUC (Fig. 4). Hmsc showed a marginally lower performance, in particular for the simulation scenario with 10% species proportion (Fig. 4 a).

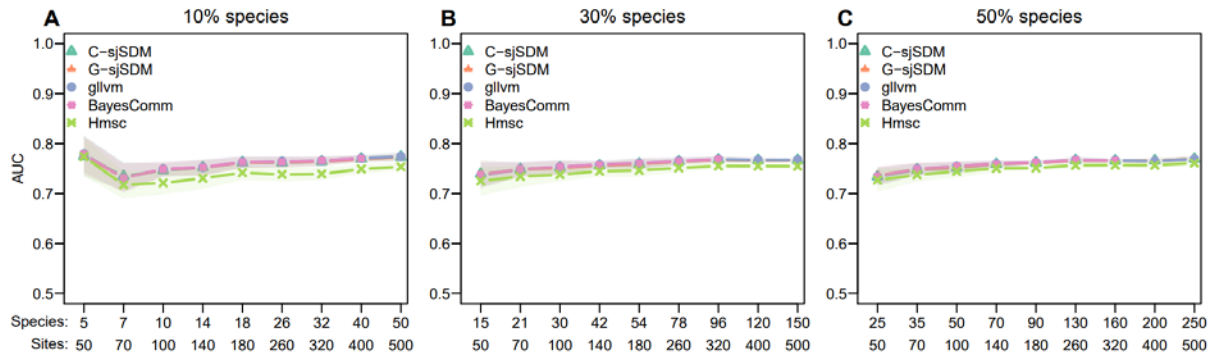


Figure 4: Results of predictive performance in simulated species distributions for G-sjSDM and C-sjSDM with gllvm, BayesComm, and Hmsc as references. Species distribution scenarios with 50 to 500 sites and 10% (a), 30% (b) and 50% (c) species were simulated, on which the models were fitted (training). Models predicted species distributions for additional 50 to 500 sites (testing). Area under the curve (AUC) was used to evaluate predictive performance on holdout.

Case Study - Inference of species-species associations from eDNA

In our eDNA case study, we found that the strongest negative species-species covariances were among the most abundant species (Fig. 5 a - c). When increasing regularization strength, positive species-species associations changed from rare to common species, while negative species-species covariances stayed constant (Fig. 5 a - c). We judged the strongest regularization of $6.5e-2$ as most appropriate (see discussion), and used the result from this model to sort species according to what environmental variables were identified as most important for them (Fig. 5d). We found that the strongest negative species-species covariances were primarily among species that responded strongly to the same environmental

covariates (Fig. 5d) and that positive species-species covariances were mostly found between species that responded strongly to different environmental covariates (Fig. 5d).

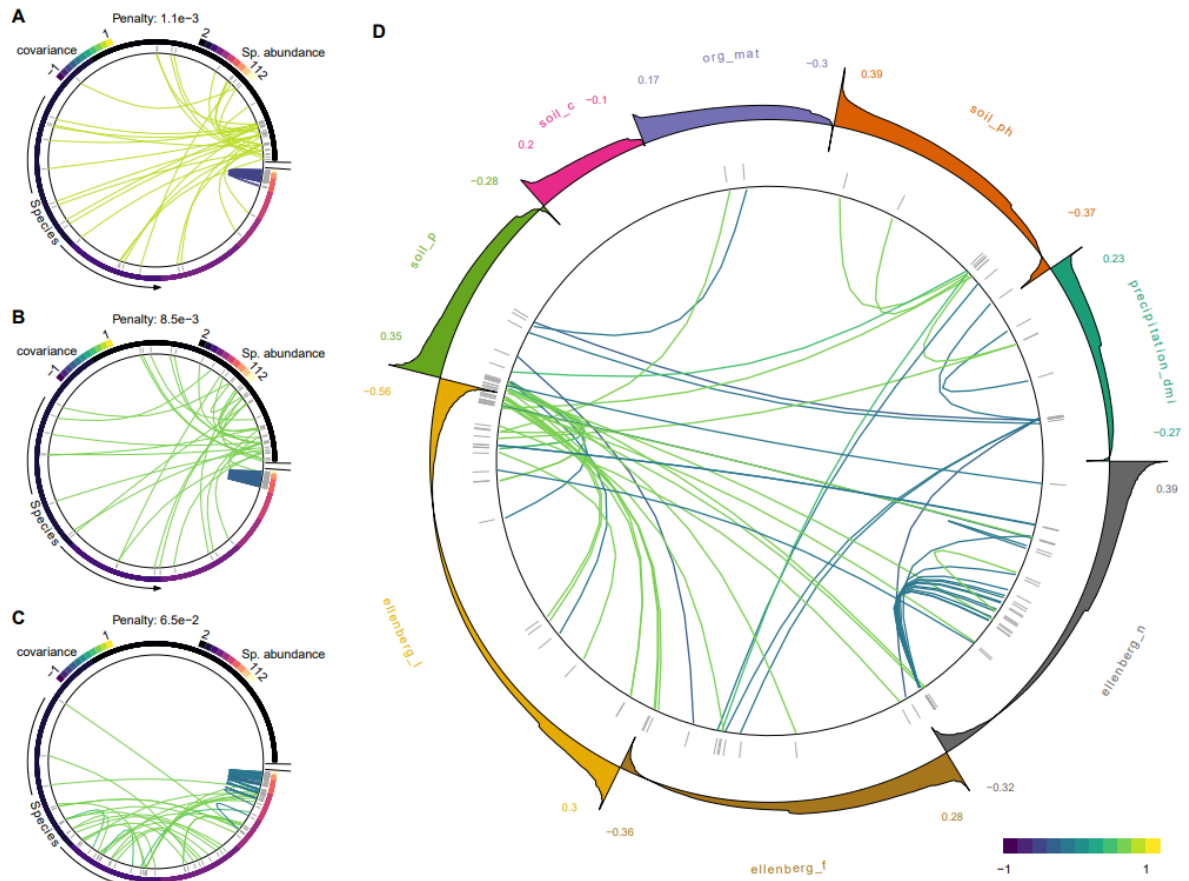


Figure 5: Inferred species associations and environmental preferences for the eDNA community data. The left column (panel A-C) shows species-species associations for different regularization penalties, with the 5564 species sorted according to their mean abundance in the 126 sites. The large panel D) shows the covariance structure of c), but with species sorted after their most important environmental coefficients (the outer ring shows the environmental effect distribution for the species within the group).

Discussion

jSDMs extend standard species distribution models by accounting also for species-species associations. A limitation of current jSDM software, however, is their slow runtimes, and possibly a tendency towards overfitting via the relatively flexible species-species association structure. In this study, we presented sjSDM, a new numerical approach for fitting jSDMs that uses Monte-Carlo integration of the model likelihood, with the option to move calculations to GPUs, and a novel approach to reduce overfitting via an elastic net regularization on the

species covariances. Our sjSDM approach is orders of magnitude faster than existing method and predicts as well as any of the other jSDM packages that we used as a benchmark. Moreover, sjSDM infers the sign of species-species associations in a wide range of scenarios better than the tested alternatives, arguably due to our more flexible regularization. Advantages over non-latent jSDMs occurred in particular for sparse species-species associations, while improvement over latent-variable were visible for all tested species-species association structures.

Computational performance

For large datasets, our sjSDM approach is orders of magnitudes faster than state-of-the-art jSDMs, especially when using GPU computations (Fig. 1a). In our benchmarks, runtimes for Hmsc, BayesComm, and gllvm started to increase exponentially when the number of species exceeded around 100 (Fig. 1a). Moreover, BayesComm and Hmsc use MCMC sampling, and our results suggest that many of those calculations for Hmsc are not fully converged (Table S2), meaning that the runtimes for a high-quality estimate might be even be higher. The exponential scaling means that present jSDM software is not suitable for the analysis of high-throughput technologies that can generate communities with thousands of species (Humphreys *et al.* 2019; Tikhonov *et al.* 2019a; Wilkinson *et al.* 2019). Our sjSDM approach, in contrast, scaled close to linearly (Fig. 1), and for GPUs, runtime depended more on the number of sites than on the number of species (Fig. 2), making it very suitable to the typical structure of eDNA data.

Accuracy in inferring the correct species associations

For data simulated with dense species-species associations (meaning that all species interact), all models showed similar performance in correctly inferring environmental responses (Fig. S2b, Fig. S2a), but the non-latent approaches sjSDM and BayesComm achieved significant higher accuracy in inferring the correct signs of species-species

associations (Fig. 3a). For sparse species-species associations (Fig. 3a), BayesComm, which had showed the best performance in correctly inferring dense species-species association structures, achieved the lowest performance, while Hmsc and gllvm performed better, but still not as well as sJSDM (Fig. 3b).

We explain these results by the fact that BayesComm's high flexibility is disadvantageous when handling sparse species-species associations, whereas the regularization imposed by the latent-variables structure is helpful in the same situation, but can also impose bias because it reduces the model's degree of freedom (see also Warton *et al.*, 2015). We note that the latent-variable approach has many analogies to the Wishart prior, which is often used to regularize covariance matrices in Bayesian statistics (e.g. Tokuda *et al.* 2011). This analogy could also help to understand the regularization bias imposed by latent-variable structure: it is known that decreasing the degrees of freedom in the Wishart prior introduces a bias on the covariance estimation that depends on the degrees of freedom of the Wishart distribution (cf. Tokuda *et al.* 2011). We believe that the LVM approach behaves analogous, with lower degrees of freedom creating more regularization, but also more bias (compare Fig. 2a, Fig. S3). MVP models such as BayesComm that fully parametrize the species-species covariance matrix do not seem to suffer from this problem (Fig. 3a), but our results suggest that they are more prone to overfitting in sparse situations (see below), apart from the fact that they scale disadvantageously with the number of species (Fig. 1a).

More generally, we believe that the accuracy of the inferred species associations, particularly in the presence of sparse associations or wide data, will depend crucially on the chosen regularization approach. Alternative regularization options, including the one chosen by us, could in principle be included in all the examined modelling approaches. Specifically, the elastic net regularization employed in our approach could also be expressed as a prior in a Bayesian model, and thus be implemented in software such as Hmsc, BayesComm. We believe that more research in this direction will be critical for making the jSDM approach

applicable for high-throughput community data, which often consists of thousands of species or OTUs on a few hundred sites (e.g. Humphreys *et al.* 2019). Without flexible regularization, models may fail to converge, or produce misleading or wrong results (see Zou & Hastie 2005).

Our case study with a real eDNA dataset underlines these points: with less or almost no regularization, our model inferred the strongest positive species-species associations between the rarest species, which is unlikely to be correct (Fig. 5a, b), since these extremely rare species carry almost no information about co-occurrences (two occurrences over 124 sites). With increasing regularization, the inferred associations structure shifted towards the more abundant species (Fig. 5 a-c), with mostly negative species-species associations that did not shift when further increasing regularization strength. For the rare species, a tendency towards positive associations remained, which is supported by an earlier finding (Calatayud *et al.* 2019). These observations overall suggest that the regularization makes misleading structures disappear while still letting true correlation structures ‘survive’.

Implications and applications of the approach for ecological data analysis

Many recent studies have stressed that jSDMs may improve predictions (e.g. Norberg *et al.* 2019), but none of these studies tested whether these improvements were made with correctly estimated parameters. From theory, one would expect that species associations are important for accurate species occurrence predictions (Dormann *et al.* 2012; Wisz *et al.* 2013; Norberg *et al.* 2019). However, our results, which show that models achieved similar predictive performance (Fig. 4), despite different accuracy in inferring species interaction structures (Fig. 3), raises the question whether the reported performance increases are due to jSDMs exploiting true interaction structures, or simply arise from the higher model complexity of jSDMs, which allows fitting the data more flexibly. Further systematic benchmarks, where model structures on biotic and abiotic predictions are flexibly adopted (e.g. via machine

learning approaches such as in Chen *et al.* 2018) could help to better understand how important biotic interactions truly are for achieving high predictive performance.

By this, we do not mean to suggest that jSDMs are of little interest for ecologists. Rather the opposite - in our view, the ecologically most interesting results of jSDMs are in the covariance estimates. They could be used, for example, to test if the strength or structure of species associations varies with space or environmental predictors; or if spatial species associations correlate with local trophic or competitive interactions or traits (see generally Poisot *et al.* 2015). For regional studies, there is the prospect of extending the traditional variation partitioning (Cottenie 2005) by biotic effects. This could be done, for example, by including spatial predictions in the jSDM (e.g. Arnqvist 2020), and then implementing a variation partitioning amongst space, biotic, and environmental predictors (e.g. Nakagawa & Schielzeth 2013). To trust all such analyses, however, we have to be sure that species-species associations are inferred correctly.

Finally, a limitation often noted is that current jSDMs, including our sjSDM, assume symmetric species-species associations (Zurell *et al.* 2018). We acknowledge that it would be useful to extend the approach to asymmetric interactions, but we believe that with the current and even new static high-throughput data this might be not feasible. If more high-resolution dynamic data becomes available, it might be possible to use causal methods that allow to infer the direction of interactions (e.g. Barraquand *et al.* 2019), which would therefore be more suitable for inferring the structure of food webs and other asymmetric species networks.

Conclusion

We presented sjSDM, a new method to fit jSDMs, and benchmarked it against state-of-the-art jSDM software. sjSDM is orders of magnitudes faster than current alternatives, and it can be flexibly regularized, which leads to overall superior performance in inferring the correct species

association structure. We provide our tool in a R package, with a simple and intuitive application programming interface and the ability to switch easily between linear and non-linear modeling, as well as between CPU and GPU computing.

Acknowledgments

We would like to thank Douglas Yu for valuable comments and suggestions.

Authors' Contributions

FH and MP jointly conceived and designed the study. MP implemented the sjSDM software, ran the experiments, and analyzed the data. Both authors contributed equally to discussing and interpreting the results, and to the preparation of the manuscript.

Data Accessibility

The compiled datasets for runtime benchmarking (case study 1) are available as supporting information for Wilkinson *et al.* 2019. The eDNA dataset is available at https://github.com/tobiasgf/man_vs_machine. The analysis and the R package sjSDM is available at <https://github.com/TheoreticalEcology/s-jSDM>.

References

- Arnqvist, G. (2020). Mixed Models Offer No Freedom from Degrees of Freedom. *Trends in Ecology & Evolution*, S0169534719303465.
- Bálint, M., Pfenninger, M., Grossart, H.-P., Taberlet, P., Vellend, M., Leibold, M.A., *et al.* (2018). Environmental DNA Time Series in Ecology. *Trends in Ecology & Evolution*, 33, 945–957.
- Barraquand, F., Picoche, C., Detto, M. & Hartig, F. (2019). Inferring species interactions using Granger causality and convergent cross mapping. *arXiv:1909.00731 [q-bio, stat]*.
- Bartholomew, D.J., Knott, M. & Moustaki, I. (2011). *Latent variable models and factor analysis: A unified approach*. John Wiley & Sons.
- Brunbjerg, A.K., Bruun, H.H., Moeslund, J.E., Sadler, J.P., Svenning, J.-C. & Ejrnæs, R. (2017). Ecospace: A unified framework for understanding variation in terrestrial biodiversity. *Basic and Applied Ecology*, 18, 86–94.
- Calatayud, J., Andivia, E., Escudero, A., Melián, C.J., Bernardo-Madrid, R., Stoffel, M., *et al.* (2019). Positive associations among rare species and their persistence in ecological assemblages. *Nature Ecology & Evolution*, 1–6.
- Chib, S. & Greenberg, E. (1998). Analysis of multivariate probit models. *Biometrika*, 85, 347–361.
- Clark, J.S., Gelfand, A.E., Woodall, C.W. & Zhu, K. (2014). More than the sum of the parts: forest climate response from joint species distribution models. *Ecological Applications*, 24, 990–999.
- Cottenie, K. (2005). Integrating environmental and spatial processes in ecological community dynamics: Meta-analysis of metacommunities. *Ecology Letters*, 8, 1175–1182.

- Cristescu, M.E. (2014). From barcoding single individuals to metabarcoding biological communities: towards an integrative approach to the study of global biodiversity. *Trends in Ecology & Evolution*, 29, 566–571.
- Deiner, K., Bik, H.M., Mächler, E., Seymour, M., Lacoursière-Roussel, A., Altermatt, F., *et al.* (2017). Environmental DNA metabarcoding: Transforming how we survey animal and plant communities. *Molecular Ecology*, 26, 5872–5895.
- Desjonquères, C., Gifford, T. & Linke, S. (n.d.). Passive acoustic monitoring as a potential tool to survey animal and ecosystem processes in freshwater environments. *Freshwater Biology*, 0.
- Dormann, C.F., Bobrowski, M., Dehling, D.M., Harris, D.J., Hartig, F., Lischke, H., *et al.* (2018). Biotic interactions in species distribution modelling: 10 questions to guide interpretation and avoid false conclusions. *Global Ecol Biogeogr*, 27, 1004–1016.
- Dormann, C.F., Schymanski, S.J., Cabral, J., Chuine, I., Graham, C., Hartig, F., *et al.* (2012). Correlation and process in species distribution models: bridging a dichotomy. *Journal of Biogeography*, 39, 2119–2131.
- Elith, J. & Leathwick, J.R. (2009). Species Distribution Models: Ecological Explanation and Prediction Across Space and Time. *Annual Review of Ecology, Evolution, and Systematics*, 40, 677–697.
- Fritzler, A., Koitka, S. & Friedrich, C.M. (2017). Recognizing Bird Species in Audio Files Using Transfer Learning, 14.
- Frøslev, T.G., Kjøller, R., Bruun, H.H., Ejrnæs, R., Hansen, A.J., Læssøe, T., *et al.* (2019). Man against machine: Do fungal fruitbodies and eDNA give similar biodiversity assessments across broad environmental gradients? *Biological Conservation*, 233, 201–212.
- Gallien, L., Douzet, R., Pratte, S., Zimmermann, N.E. & Thuiller, W. (2012). Invasive species distribution models – how violating the equilibrium assumption can create new insights. *Global Ecology and Biogeography*, 21, 1126–1136.

- Gilbert, B. & Bennett, J.R. (2010). Partitioning variation in ecological communities: do the numbers add up? *Journal of Applied Ecology*, 47, 1071–1082.
- Golding, N. & Harris, D.J. (2015). *BayesComm: Bayesian community ecology analysis*.
- Golding, N., Nunn, M.A. & Purse, B.V. (2015). Identifying biotic interactions which drive the spatial distribution of a mosquito community. *Parasites & Vectors*, 8, 367.
- Guirado, E., Tabik, S., L. Rivas, M., Alcaraz-Segura, D. & Herrera, F. (2018). Automatic whale counting in satellite images with deep learning. *bioRxiv*.
- Hui, F.K.C. (2016). boral – Bayesian Ordination and Regression Analysis of Multivariate Abundance Data in r. *Methods in Ecology and Evolution*, 7, 744–750.
- Humphreys, J.M., Murrow, J.L., Sullivan, J.D. & Prosser, D.J. (2019). Seasonal occurrence and abundance of dabbling ducks across the continental United States: Joint spatio-temporal modelling for the Genus *Anas*. *Diversity and Distributions*, 25, 1497–1508.
- Krapu, C. & Borsuk, M. (2020). A spatial community regression approach to exploratory analysis of ecological data. *Methods in Ecology and Evolution*, n/a.
- Lasseck, M. (2018). Audio-based bird species identification with deep convolutional neural networks. *Working Notes of CLEF*, 2018.
- Leibold, M.A. & Chase, J.M. (2017). *Metacommunity ecology*. Princeton University Press.
- Leibold, M.A., Holyoak, M., Mouquet, N., Amarasekare, P., Chase, J.M., Hoopes, M.F., *et al.* (2004). The metacommunity concept: a framework for multi-scale community ecology. *Ecology Letters*, 7, 601–613.
- Levine, J.M., Bascompte, J., Adler, P.B. & Allesina, S. (2017). Beyond pairwise mechanisms of species coexistence in complex communities. *Nature*, 546, 56–64.
- Mac Aodha, O., Gibb, R., Barlow, K.E., Browning, E., Firman, M., Freeman, R., *et al.* (2018). Bat detective—Deep learning tools for bat acoustic signal detection. *PLOS Computational Biology*, 14, e1005995.
- Mainali, K.P., Warren, D.L., Dhileepan, K., McConnachie, A., Strathie, L., Hassan, G., *et al.* (2015). Projecting future expansion of invasive species: comparing and improving

- methodologies for species distribution modeling. *Global Change Biology*, 21, 4464–4480.
- Mittelbach, G.G. & Schemske, D.W. (2015). Ecological and evolutionary perspectives on community assembly. *Trends in Ecology & Evolution*, 30, 241–247.
- Nakagawa, S. & Schielzeth, H. (2013). A general and simple method for obtaining R² from generalized linear mixed-effects models. *Methods in Ecology and Evolution*, 4, 133–142.
- Niku, J., Brooks, W., Herliansyah, R., Hui, F.K.C., Taskinen, S. & Warton, D.I. (2020). *gllvm: Generalized linear latent variable models*.
- Niku, J., Hui, F.K.C., Taskinen, S. & Warton, D.I. (2019). gllvm: Fast analysis of multivariate abundance data with generalized linear latent variable models in r. *Methods in Ecology and Evolution*, n/a.
- Norberg, A., Abrego, N., Blanchet, F.G., Adler, F.R., Anderson, B.J., Anttila, J., *et al.* (2019). A comprehensive evaluation of predictive performance of 33 species distribution models at species and community levels. *Ecological Monographs*, 0, e01370.
- Ovaskainen, O., Hottola, J. & Siitonen, J. (2010). Modeling species co-occurrence by multivariate logistic regression generates new hypotheses on fungal interactions. *Ecology*, 91, 2514–2521.
- Ovaskainen, O., Tikhonov, G., Norberg, A., Blanchet, F.G., Duan, L., Dunson, D., *et al.* (2017). How to make more out of community data? A conceptual framework and its implementation as models and software. *Ecology Letters*, 20, 561–576.
- Peres-Neto, P.R. & Legendre, P. (2010). Estimating and controlling for spatial structure in the study of ecological communities. *Global Ecology and Biogeography*, 19, 174–184.
- Picciulin, M., Kéver, L., Parmentier, E. & Bolgan, M. (2019). Listening to the unseen: Passive acoustic monitoring reveals the presence of a cryptic fish species. *Aquatic Conservation: Marine and Freshwater Ecosystems*, 29, 202–210.

- Poisot, T., Stouffer, D.B. & Gravel, D. (2015). Beyond species: why ecological interaction networks vary through space and time. *Oikos*, 124, 243–251.
- Pollock, L.J., Tingley, R., Morris, W.K., Golding, N., O'Hara, R.B., Parris, K.M., *et al.* (2014). Understanding co-occurrence by modelling species simultaneously with a Joint Species Distribution Model (JSDM). *Methods in Ecology and Evolution*, 5, 397–406.
- Skrondal, A. & Rabe-Hesketh, S. (2004). *Generalized latent variable modeling: Multilevel, longitudinal, and structural equation models*. Chapman and Hall/CRC.
- Tabak, M.A., Norouzzadeh, M.S., Wolfson, D.W., Sweeney, S.J., Vercauteren, K.C., Snow, N.P., *et al.* (2019). Machine learning to classify animal species in camera trap images: Applications in ecology. *Methods in Ecology and Evolution*, 10, 585–590.
- Thuiller, W., Lavorel, S., Sykes, M.T. & Araújo, M.B. (2006). Using niche-based modelling to assess the impact of climate change on tree functional diversity in Europe. *Diversity and Distributions*, 49–60.
- Tikhonov, G., Abrego, N., Dunson, D. & Ovaskainen, O. (2017). Using joint species distribution models for evaluating how species-to-species associations depend on the environmental context. *Methods in Ecology and Evolution*, 8, 443–452.
- Tikhonov, G., Duan, L., Abrego, N., Newell, G., White, M., Dunson, D., *et al.* (2019a). Computationally efficient joint species distribution modeling of big spatial data. *Ecology*, n/a, e02929.
- Tikhonov, G., Ovaskainen, O., Oksanen, J., de Jonge, M., Opedal, O. & Dallas, T. (2019b). *Hmsc: Hierarchical model of species communities*.
- Tobler, M.W., Kéry, M., Hui, F.K.C., Guillera-Aroita, G., Knaus, P. & Sattler, T. (2019). Joint species distribution models with species correlations and imperfect detection. *Ecology*, 100, e02754.
- Tokuda, T., Goodrich, B., Van Mechelen, I., Gelman, A. & Tuerlinckx, F. (2011). Visualizing distributions of covariance matrices. *Columbia Univ., New York, USA, Tech. Rep*, 18–18.

- Urban, M.C., Bocedi, G., Hendry, A.P., Mihoub, J.-B., Pe'er, G., Singer, A., *et al.* (2016). Improving the forecast for biodiversity under climate change. *Science*, 353.
- Van der Putten, W.H., Macel, M. & Visser, M.E. (2010). Predicting species distribution and abundance responses to climate change: why it is essential to include biotic interactions across trophic levels. *Philosophical Transactions of the Royal Society B: Biological Sciences*, 365, 2025–2034.
- Warton, D.I., Blanchet, F.G., O'Hara, R.B., Ovaskainen, O., Taskinen, S., Walker, S.C., *et al.* (2015). So Many Variables: Joint Modeling in Community Ecology. *Trends in Ecology & Evolution*, 30, 766–779.
- Wilkinson, D.P., Golding, N., Guillera-Arroita, G., Tingley, R. & McCarthy, M.A. (2019). A comparison of joint species distribution models for presence–absence data. *Methods in Ecology and Evolution*, 10, 198–211.
- Wisz, M.S., Pottier, J., Kissling, W.D., Pellissier, L., Lenoir, J., Damgaard, C.F., *et al.* (2013). The role of biotic interactions in shaping distributions and realised assemblages of species: implications for species distribution modelling. *Biological Reviews*, 88, 15–30.
- Wood, C.M., Gutiérrez, R.J. & Peery, M.Z. (2019). Acoustic monitoring reveals a diverse forest owl community, illustrating its potential for basic and applied ecology. *Ecology*, 100, e02764.
- Wrege, P.H., Rowland, E.D., Keen, S. & Shiu, Y. (2017). Acoustic monitoring for conservation in tropical forests: examples from forest elephants. *Methods in Ecology and Evolution*, 8, 1292–1301.
- Zou, H. & Hastie, T. (2005). Regularization and variable selection via the elastic net. *Journal of the Royal Statistical Society: Series B (Statistical Methodology)*, 67, 301–320.

Appendix

Simulation scenarios

The MVP can be interpreted as individual GLMs connected by correlated residuals, which are sampled from a multivariate Gaussian, and with a probit link. Sites are notated with $i = 1, \dots, M$; species with $j = 1, \dots, K$; and environmental covariates with $n = 1, \dots, N$. Environmental covariates and species responses (beta) were uniformly sampled (1,2). The lower triangular covariance matrix was uniformly sampled (3), the diagonal was set to one (4) and multiplied by the transposed lower triangular to get a symmetric positive definite matrix (4).

$$\beta, X \sim U(-1, +1)$$

(1)

$$\Sigma_{j,j}^{lower} \sim U(-1, +1)$$

(2)

$$\Sigma_{j=j}^{lower} = 1$$

(3)

$$\Sigma_{j,j} = \Sigma * \Sigma^t$$

(4)

$$y_{ij} = X_{in} * \beta_{nj} + MVN(0; \Sigma_{jj})$$

(5)

$$z_{ij} = 1 (y_{ij} > 0)$$

(6)

Species responses consist of a linear species - environmental response and correlated residuals (5). Following a probit link, responses higher than zero were set to one and the remaining to 0.

Model settings and computer setup

This section provides a more detailed explanation about model settings and the computer setup under which our benchmarks were performed (See Table S1 for an overview). Unless stated otherwise, we used default settings for parameters.

Table S1: Overview of the used approaches

| Model | Optimization type | Package |
|---------------------------|---|-----------|
| Multivariate probit model | MLE | sjSDM |
| | MCMC | BayesComm |
| Latent-variable model | MCMC | Hmsc |
| | Variational bayes / Laplace approximation | gllvm |

BayesComm

BayesComm models were fit in 50,000 MCMC sampling iterations, with two chains, thinning = 50, and burn-in of 5000. Prior were not changed from default: normal prior on regression coefficients $b \sim N(0;10)$ and an inverse Wishart prior on the covariance matrix.

Hmsc

Hmsc models were fit in 50,000 MCMC sampling iterations, with two chains, thinning = 50, and burn-in of 5000. Since the two chains were not run in parallel (which is supported by Hmsc), the measured runtime was halved. The number of latent variables in Hmsc are automatically inferred by gamma shrinkage prior. The shrinkage priors of Hmsc were not changed from default.

We note that there is the option to tune regularization via shrinkage priors in Hmsc: a_1 regularizes the lower triangular of the species association and a_2 regularizes the number of

latent variables (see Bhattacharya & Dunson 2011). We acknowledge that this might improve accuracy of HMSC inference. On the other hand, it should be noted that a) these settings were not tuned in recent benchmarks, and are likely not tuned by users either. b) the runtime of tuning several combinations would be not practicable (see our results) and c) it is to be expected that a low a_2 results in a higher accuracy but then the LVM approach would approximate the MVP model and that would contradict the LVM's unique characteristic.

gllvm

gllvm models were fit as binomial models with probit link. The number of latent variables were increased from 2 to 6 with the number of species. If default starting values = “res” caused an error, model was re-run with starting values = “zero” and if another error occurred, the model was re-run with starting values = “random”. Run time was measured individually, not as a sum over possible model fitting tries.

sjSDM

sjSDM models were fit in 50 iterations (epochs) and a batch size of 10% number of sites. Learning rate was set to 0.01. 50% number of species were set as degree of freedom (df) for covariance parametrization and the df was set to the number of species for sparse species associations.

Computer setup

All the computations were performed on the same workstation (two Intel Xeon Gold 6128 CPU @3.40 GHz) and the number of cores and threads were restricted to 6. GPU computations were carried out on a NVIDIA RTX 2080 Ti. All CPU models had access to 192 GB RAM and the GPU models to 11 GB GPU RAM). Analyses were conducted with the statistical software

R and Python (Python Software Foundation. Python Language Reference, version 3.8.1. Available at <http://www.python.org>)

Convergence check

To check convergence of sigma and the betas, the potential scale reduction factors (psrf) for Hmsc and BayesComm in the simulation scenarios were calculated (two chains, burn-in = 5000 and 50,000 sampling iterations). We found no psrf > 1.2 for BayesComm, but for all simulation scenarios at least for one parameter (beta or sigma) a psrf > 1.2 for Hmsc (Table S2).

Table S2: Rate of weights in percent with potential scale reduction factor > 1.2 in non-sparse and sparse simulation scenarios.

| Hmsc | Hmsc – Sparse associations | Number of sites | Number of species |
|-------|----------------------------|-----------------|-------------------|
| 0.08 | 0.091 | 50 | 5 |
| 0.076 | 0.075 | 70 | 7 |
| 0.055 | 0.096 | 100 | 10 |
| 0.056 | 0.108 | 140 | 14 |
| 0.047 | 0.144 | 180 | 18 |
| 0.121 | 0.13 | 260 | 26 |
| 0.112 | 0.199 | 320 | 32 |
| 0.11 | 0.195 | 400 | 40 |
| 0.076 | 0.136 | 500 | 50 |
| 0.093 | 0.072 | 50 | 15 |
| 0.043 | 0.076 | 70 | 21 |
| 0.084 | 0.094 | 100 | 30 |
| 0.081 | 0.077 | 140 | 42 |
| 0.088 | 0.101 | 180 | 54 |
| 0.053 | 0.105 | 260 | 78 |
| 0.108 | 0.133 | 320 | 96 |

| | | | |
|-------|-------|-----|-----|
| 0.066 | 0.178 | 400 | 120 |
| 0.231 | 0.154 | 500 | 150 |
| 0.053 | 0.083 | 50 | 25 |
| 0.062 | 0.044 | 70 | 35 |
| 0.064 | 0.051 | 100 | 50 |
| 0.064 | 0.1 | 140 | 70 |
| 0.08 | 0.095 | 180 | 90 |
| 0.077 | 0.141 | 260 | 130 |
| 0.107 | 0.146 | 320 | 160 |
| 0.246 | 0.124 | 400 | 200 |
| 0.227 | 0.152 | 500 | 250 |

Additional results

Scaling of the algorithms in log plots

In the main paper, we provide the benchmarks on a linear scale. Below, we also provide then in log format, which demonstrates that many other software packages, including the CPU version of sjSDM scale exponentially, while G-sjSDM scales sub-exponentially for the scenarios that we tested (Fig S1).

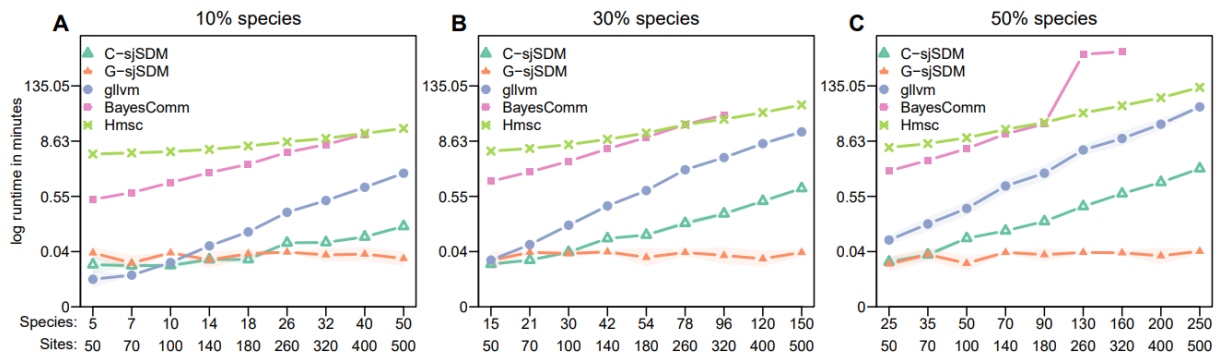


Figure S1: Results for computational log runtime benchmarking of G-sjSDM, C-sjSDM, glvm, BayesComm, and Hmsc jSDM implementations. Models were fit to different simulated SDM scenarios: 50 to 500 sites with 10% (a), 30% (b) and 50% (c) number of species (e.g. for 100 sites and 10% we get 10 species). For each scenario, ten simulations were sampled, and results were averaged. Due to high runtimes, runs for BayesComm, glvm and Hmsc were aborted at specific points.

Accuracy of inferring environmental parameters

For non-sparse species-species associations, all models inferred with high accuracy true signs of the environmental predictors and also achieved similar RMSE errors estimated environmental parameters (Fig. S2 a-b).

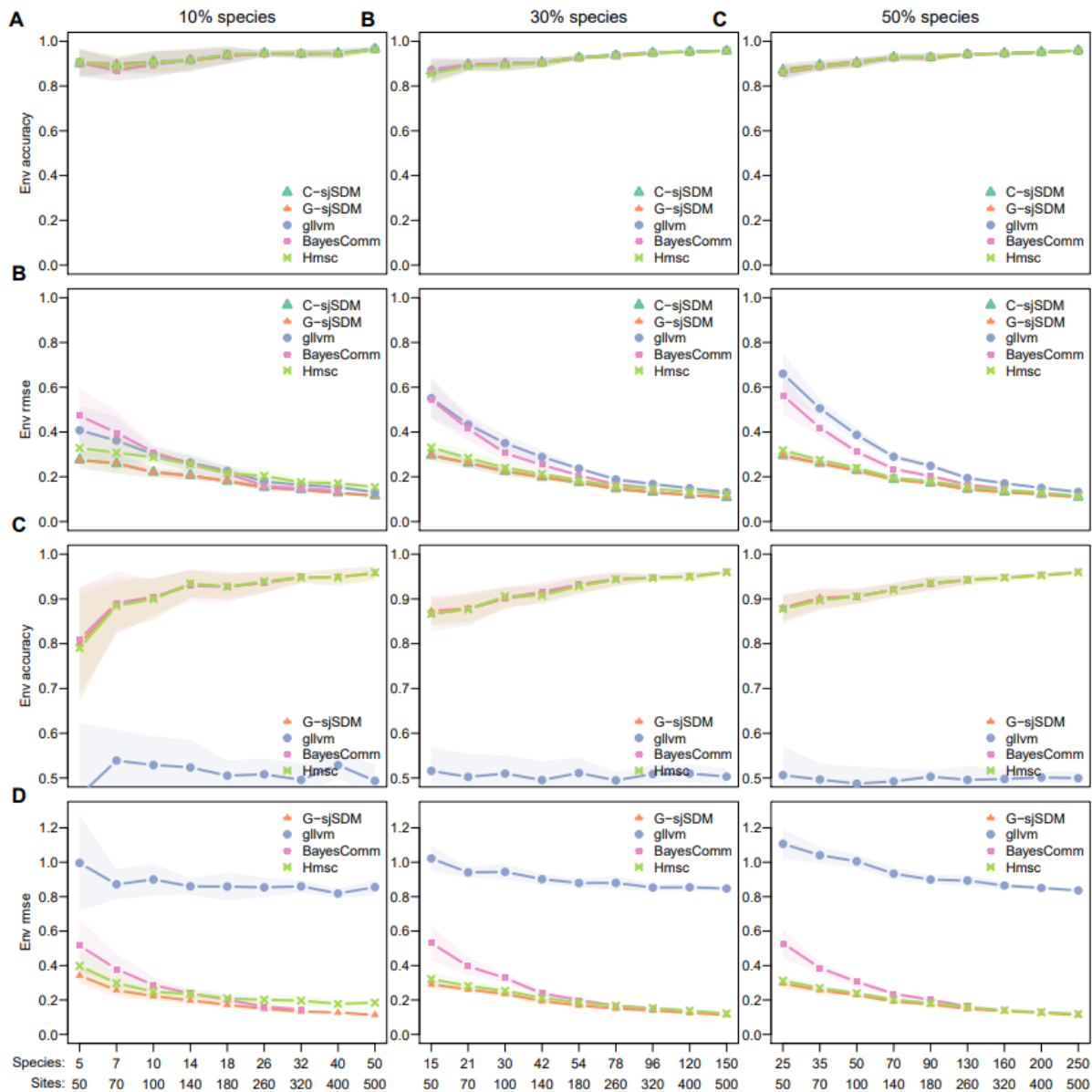


Figure S2: Results for inferential benchmarking of G-sjSDM with gllvm, BayesComm, and Hmsc as references.

Models were fit to different simulated SDM scenarios: 50 to 500 sites with 10%, 30% and 50% number of species (e.g. for 100 sites and 10% we get 10 species). For each scenario, ten simulations were sampled, and results were averaged. Due to high runtimes, runs for BayesComm, gllvm and Hmsc were aborted at specific points. A) and B) show the environmental coefficient accuracy (matching signs) and the corresponding RMSE with full species-

species association matrices. C) and D) show the environmental coefficient accuracy (matching signs) and the corresponding RMSE with sparse (50% sparsity) species-species association matrices.

For sparse species associations, the models except for gllvm achieved similar performances in inferring the environmental parameters (Fig. S2 c-d). gllvm achieved significant lower accuracy in finding the true signs of environmental parameters (Fig. S2c) and a several times higher RMSE error for environmental parameters than the other models (Fig. S2d).

Covariance accuracy behavior

To further assess the jSDM's behavior in inferring the species-species association matrix, we set the number of species to 50 and increased the number of sites from 50 to 330. For each, step we computed the averaged (we sampled 5 scenarios for each setting) covariance accuracy and environmental RMSE.

BayesComm achieved at 330 sites around 0.82 accuracy and sjSDM around 0.80. sjSDM and BayesComm increased the covariance accuracy steadily with the number of sites, while Hmsc and gllvm stopped increasing their accuracy at around 0.68 accuracy (Fig. S3 a). sjSDM and BayesComm achieved in average 0.1 more accuracy than Hmsc and gllvm (Fig. S3 a).

All models achieved a similar RMSE over all scenarios (Fig. S3 b). sjSDM showed overall the highest RMSE (Fig. S3 b). All models decreased their RMSE with increasing number of sites (Fig. S3 b).

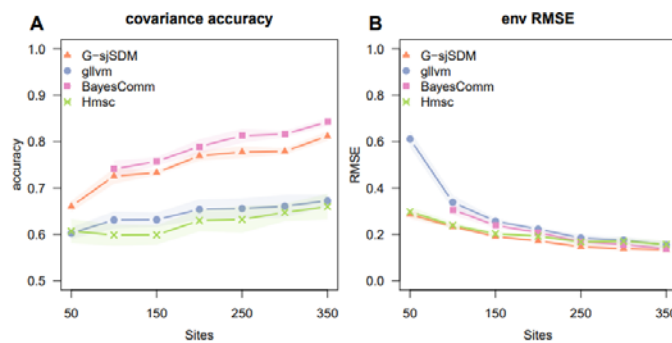


Figure S3: Results for examining the ability to recover the covariance structure in dependence of number of sites for G-sjSDM, BC, gllvm, and Hmsc. In the simulated species distribution scenarios, the number of species were constantly set to 50, but the number of sites were varied from 50 to 330 sites.

Performance was measured by the accuracy of matching signs between estimated covariances matrices and true

covariance matrices (A). Moreover, the root mean squared error for the environmental effects with the true coefficients were calculated (B). Asterisks refer to convergence issues (scale factor > 1.2 in any lambda or beta estimates)

Case Study – Inference of species-species associations

We tested several different regularization strategies: i) regularization only on covariances in species-species association matrix (elastic net, $\alpha = 0.5$ with regularization strength ranging from $3.8e-6$ to 0.5). ii) regularization on covariances in species-species association matrix and the environmental coefficients (elastic net, $\alpha = 0.5$ with regularization strength ranging from $3.8e-6$ to 0.5 . Same strength on covariances and coefficients). iii) regularization on covariances in species-species association matrix and the environmental coefficients (elastic net, $\alpha = 0.5$ with regularization strength ranging from $3.8e-6$ to 0.5 on covariances and $3.8e-5$ and 5 on environmental covariates). iv) regularization on covariances in species-species association matrix and the environmental coefficients (elastic net, $\alpha = 0.5$ with regularization strength ranging from $3.8e-6$ to 0.5 on covariances and $1.9e-5$ and 25 on environmental covariates).

To better understand the influence of regularization behavior, we computed turn-over rates. The turn-over rate ranges between $0 - 1$ and describes whether the lowest negative and highest positive 30, 300 and 300 positive covariances are the same compared to the previous regularization step (Fig. S4).

Results for different regularization strategies

We found that the $1 - \text{turnover rates}$ were similar for all regularization strategies (Fig. S4). The regularization strategies differ only in the regularization of the environmental coefficients. Thus, the additional regularization seems to have no effect on the species-species covariance regularization. The common absolute sum of the diagonals and off-diagonals of the species-species association matrix show the same structure (Fig. S6, S7).

Turnover rates for the different regularization strategies started to increase (decrease in Fig. S5 because the plots show 1- turnover rates) around 0.001 regularization strength (Fig. S5). We speculate that is the point where the regularization starts to find an optimum with important covariances.

When the regularization gets too strong, even important covariances are lost and the turnover rates starts to decrease (increase in Fig. S4) again. Also, the environmental coefficients are pushed to zero (Fig. S6).

We partitioned also the overall loss into the model's loss and the regularization loss (Fig. S5, the elastic net loss of covariances and environmental coefficients).

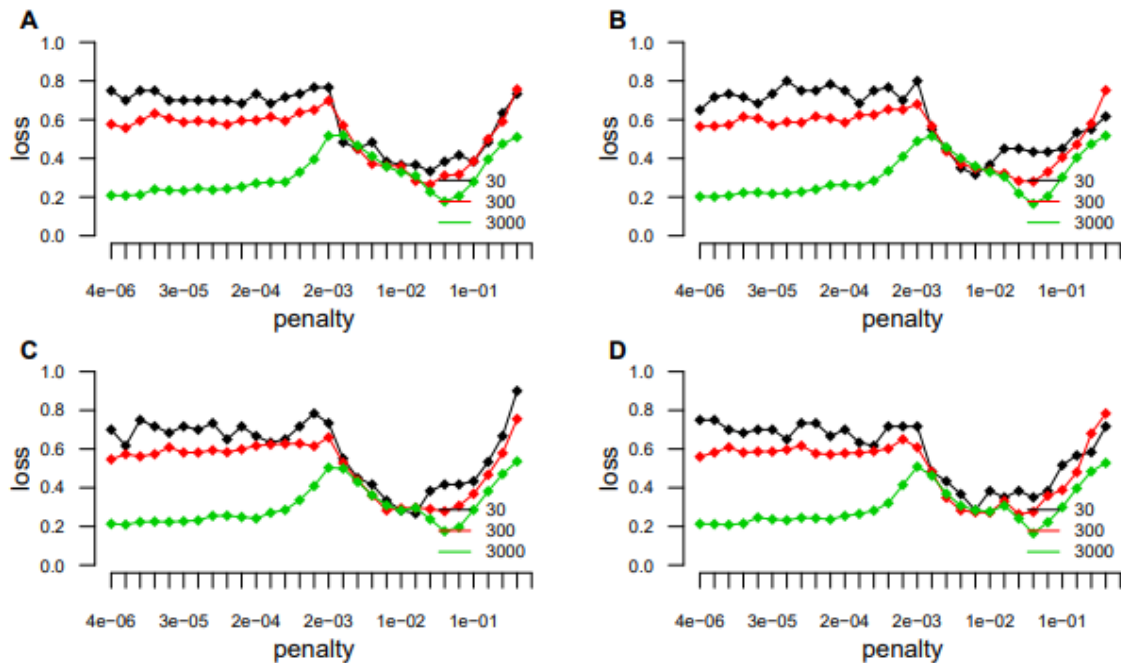


Figure S4: Turnover results for the elastic net analysis of the empirical community data generated by eDNA. The turn-over rate ranges between 0 - 1 and describes whether the lowest negative and highest positive 30, 300 and 300 positive covariances are the same compared to the previous regularization step (plotted as 1- turnover rates). Turnover rates were calculated for strongest 30 (black), 300 (red), and 3000 (green) covariances. A – C are the results for the 4 scenarios with different regularization strategies (see earlier section).

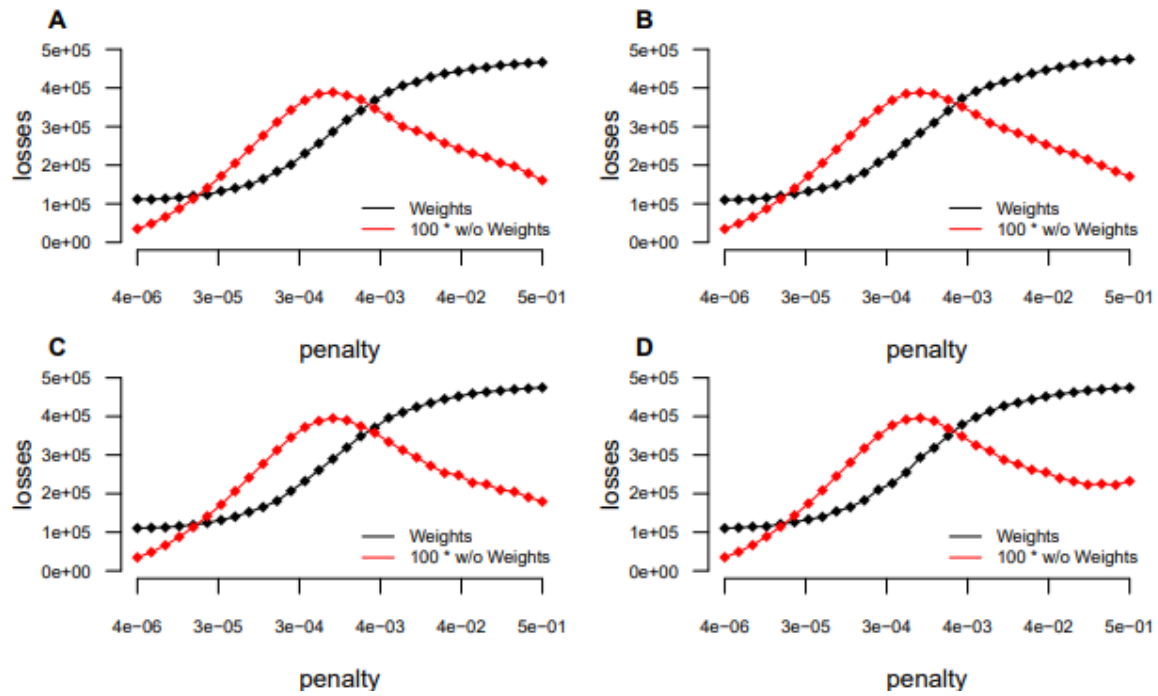


Figure S5: Loss composition for the different regularization strategies. The overall loss is composed of the loss without the regularization loss (red) and the regularization loss (black). A – C shows the results for the different regularization strategies.

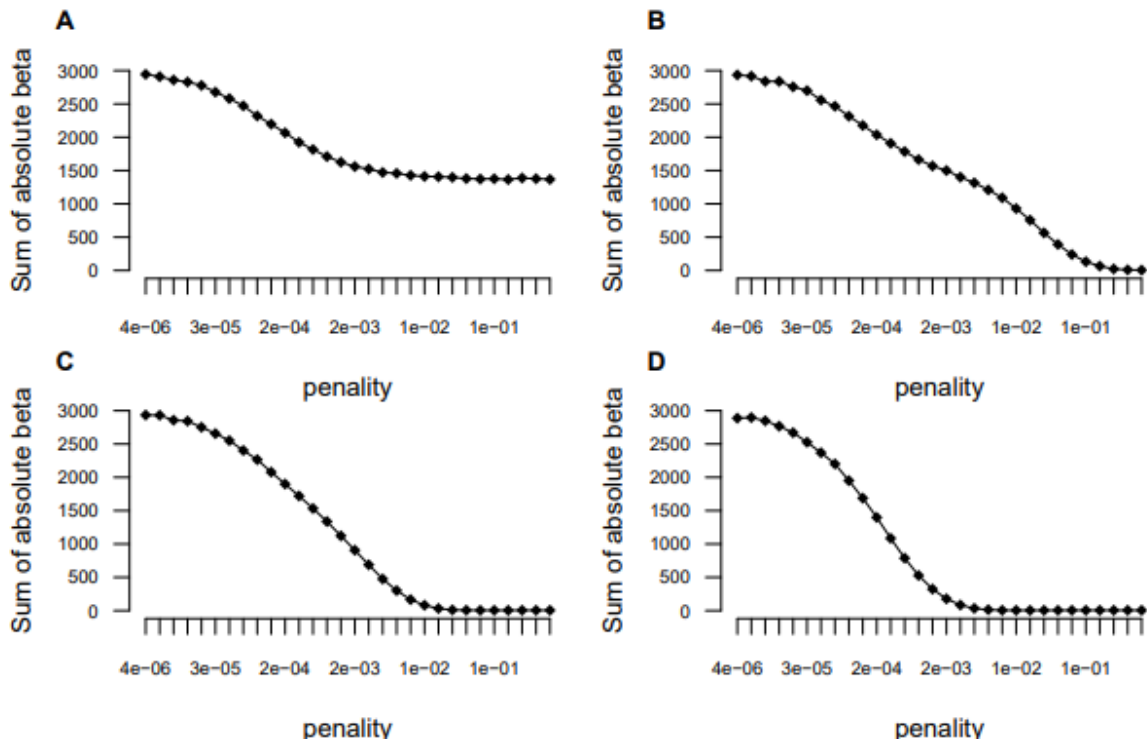


Figure S6: Sum of absolute environmental (beta) coefficients over the regularization steps. A – C shows the different regularization strategies.

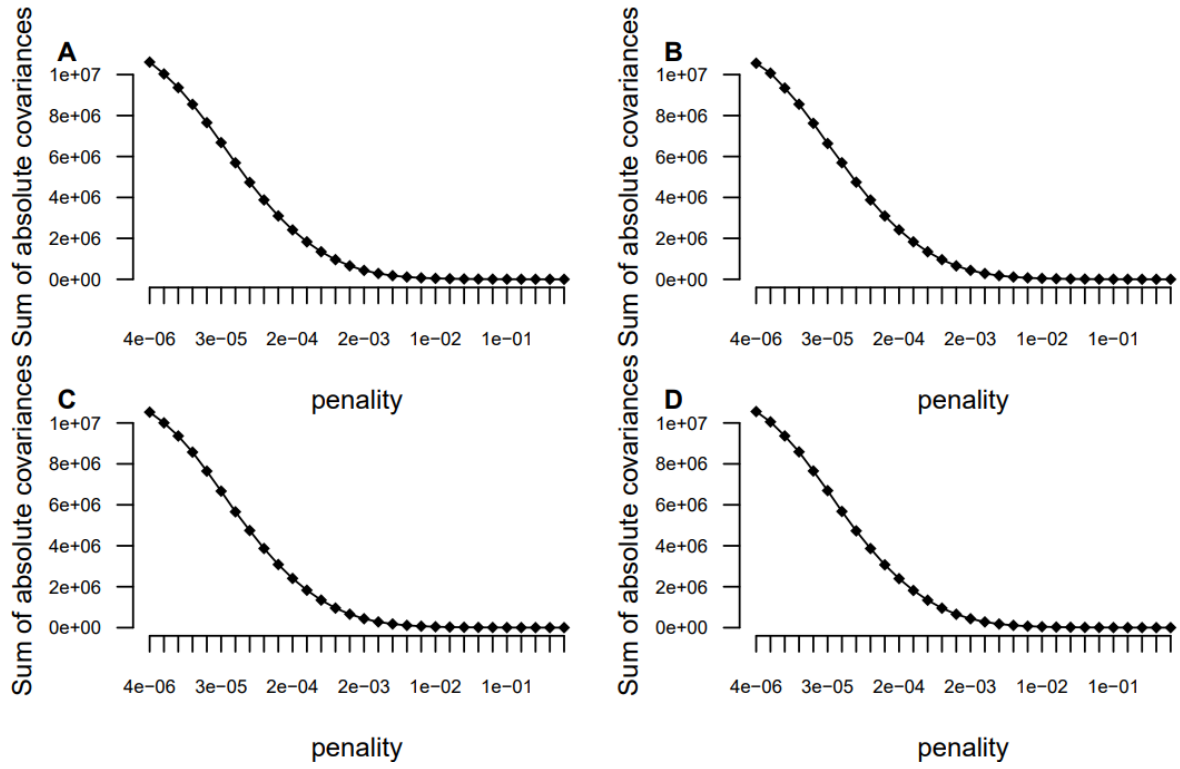


Figure S7: Sum of absolute covariances over the regularization steps. A – C shows the different regularization strategies.

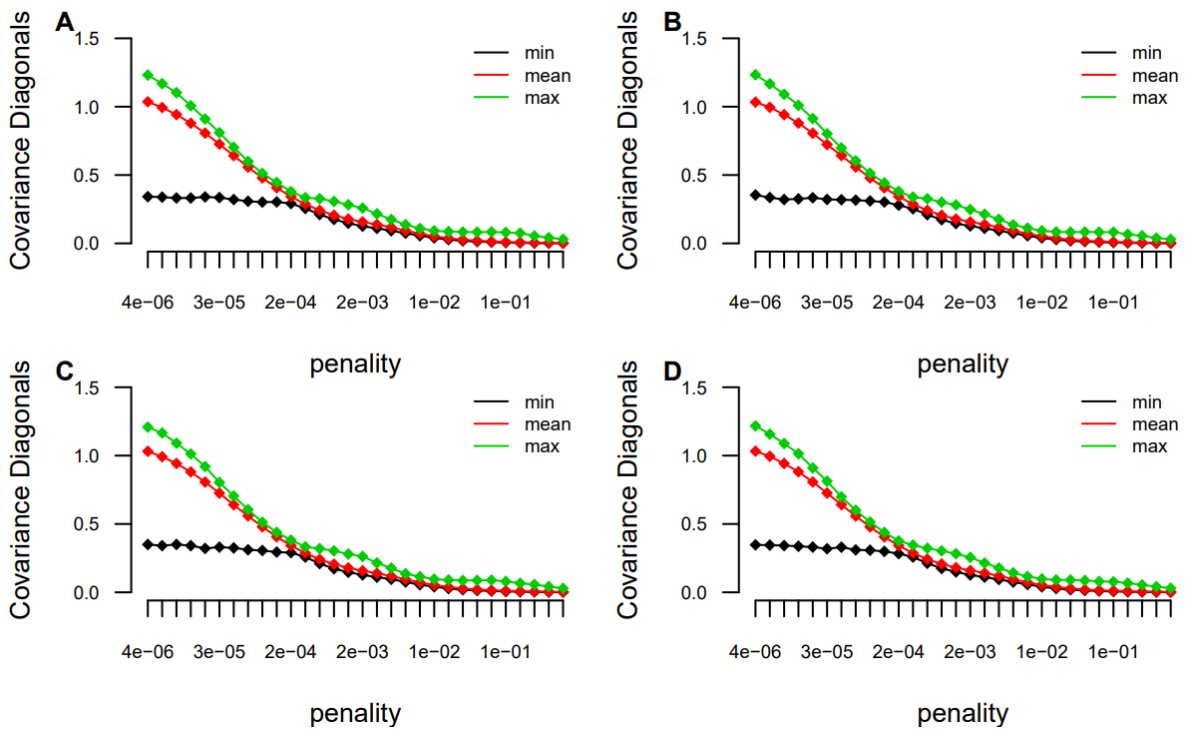


Figure S8: Mean (red), max (green), and min (black) of diagonal covariances of the species-species association matrix. A – C show the different regularization strategies.

Species-species associations for different regularization strategies

The turnover results and the overall loss composition indicate that i) the environmental regularization influences the covariance structure and ii) after around 0.001 regularization strength, important and maybe true covariances were identified.

We found in all regularization strategies similar covariance structures (Fig. S9 – S11).

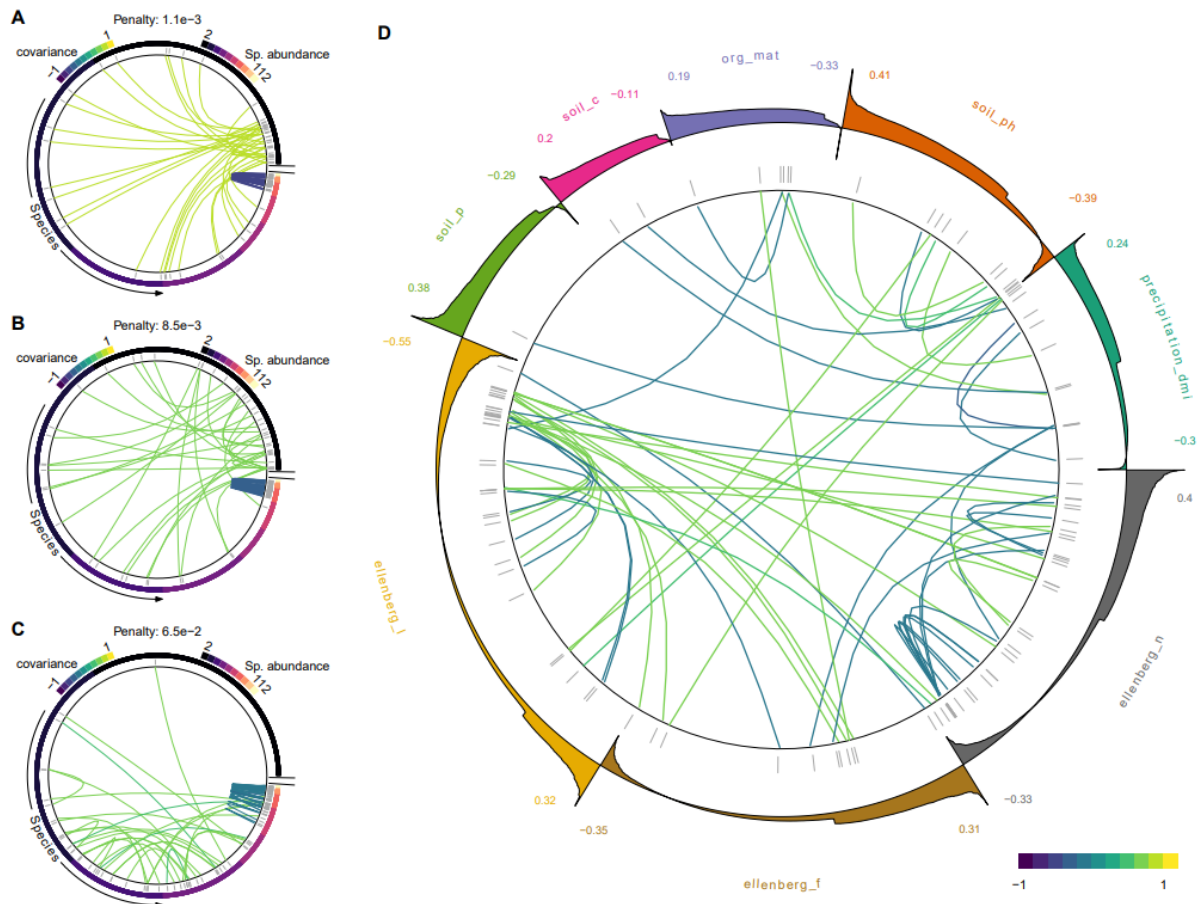


Figure S9: Results for the eDNA generated community with the first regularization strategy (no regularization for environmental coefficients). The penalty for the elastic net in the model was varied from 6e-6 to 0.5. a) – c) shows the covariance strengths for the 30 largest and 30 lowest covariances for 1.1e-3, 8.5e-3, and 6.5e-2 penalties. The 5564 species were sorted after their overall abundance over the 126 sites. D) shows the covariance structure of c), but with species sorted after their most important environmental coefficients (the outer ring shows the environmental effect distribution for the species within the group).

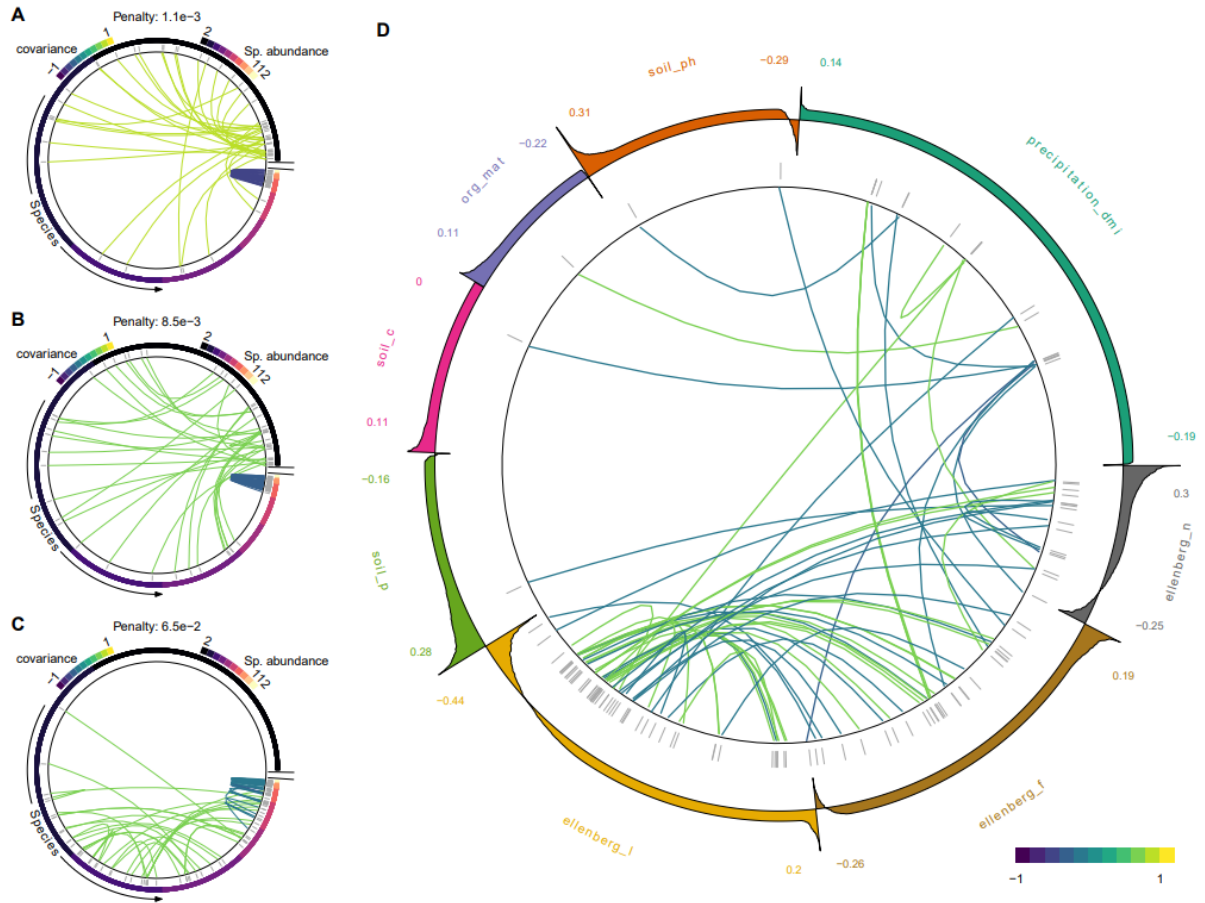


Figure S10: Results for the eDNA generated community with the first regularization strategy (stronger ($\times 10$) regularization on environmental coefficients). The penalty for the elastic net in the model was varied from 6×10^{-6} to 0.5. a) – c) shows the covariance strengths for the 30 largest and 30 lowest covariances for 1.1×10^{-3} , 8.5×10^{-3} , and 6.5×10^{-2} penalties. The 5564 species were sorted after their overall abundance over the 126 sites. D) shows the covariance structure of c), but with species sorted after their most important environmental coefficients (the outer ring shows the environmental effect distribution for the species within the group).

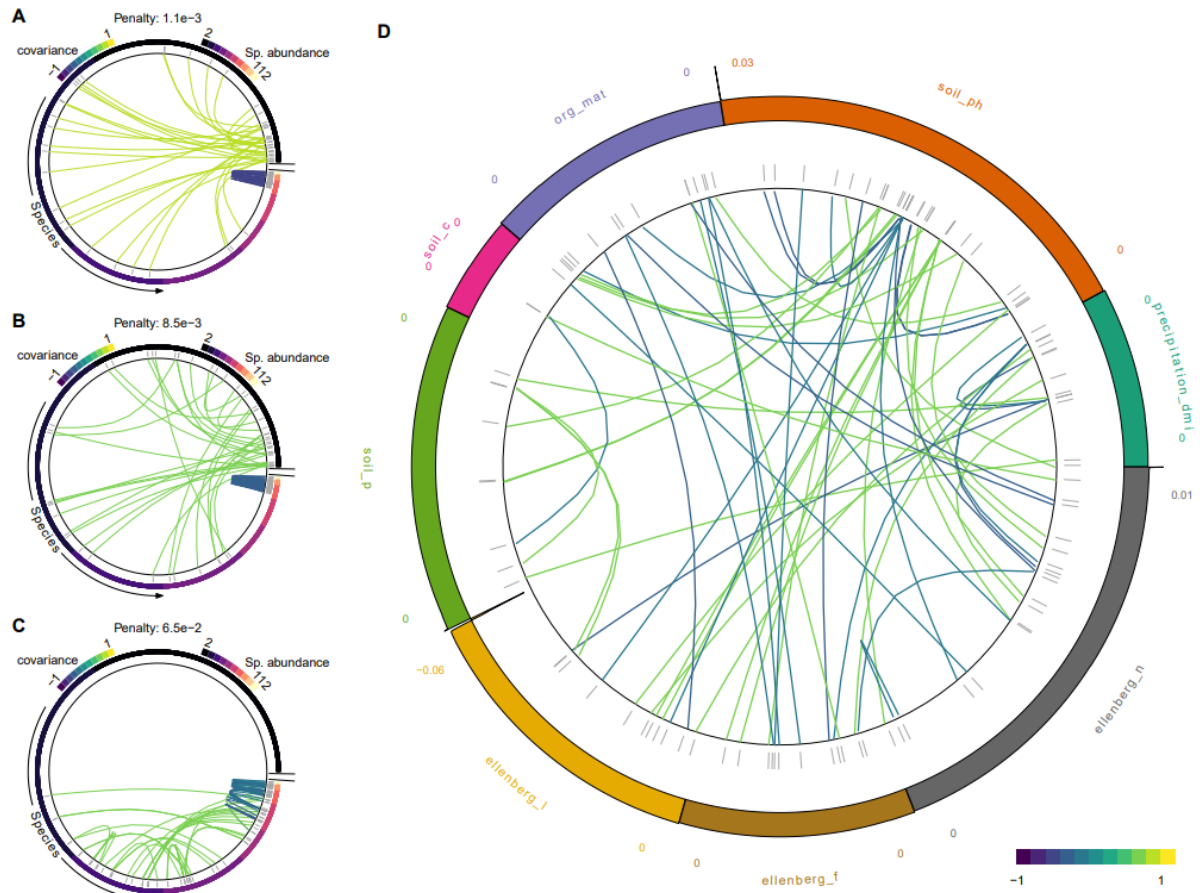


Figure S11: Results for the eDNA generated community with the first regularization strategy (very strong regularization (x50) on environmental coefficients). The penalty for the elastic net in the model was varied from 6×10^{-6} to 0.5. a) – c) shows the covariance strengths for the 30 largest and 30 lowest covariances for 1.1×10^{-3} , 8.5×10^{-3} , and 6.5×10^{-2} penalties. The 5564 species were sorted after their overall abundance over the 126 sites. D) shows the covariance structure of c), but with species sorted after their most important environmental coefficients (the outer ring shows the environmental effect distribution for the species within the group).